

Study of ^{45}Ar through (d, p) reaction at SPIRAL

L Gaudefroy¹, O Sorlin², D Beaulieu¹, Y Blumenfeld¹, Z Dombrádi³,
S Fortier¹, S Franchou¹, M Gélin², J Gibelin¹, S Grévy², F Hammache¹,
F Ibrahim¹, K Kemper⁴, K L Kratz⁵, S M Lukyanov⁶, C Monrozeau¹,
L Nalpas⁷, F Nowacki⁸, A N Ostrowski⁵, Yu-E Penionzhkevich⁶,
E Pollaco⁷, P Roussel-Chomaz², E Rich¹, J A Scarpaci¹, M G St Laurent²,
D Sohler³, M Stanoiu¹, E Trygggestad¹ and D Verney¹

¹ IPN, IN2P3-CNRS, F-91406 Orsay Cedex, France

² GANIL, BP 55027, F-14076 Caen Cedex 5, France

³ Institute of Nuclear Research, H-4001 Debrecen, Pf. 51, Hungary

⁴ Department of Physics, Florida State University, Tallahassee, FL 32306, USA

⁵ Institut für Kernchemie, Universität Mainz, D-55128 Mainz, Germany

⁶ FLNR/JINR, 141980 Dubna, Moscow region, Russia

⁷ CEA-Saclay, DAPNIA-SPhN, F-91191 Gif sur Yvette Cedex, France

⁸ IReS, Univ. Louis Pasteur, BP 28, F-67037 Strasbourg Cedex, France

Received 21 March 2005

Published 12 September 2005

Online at stacks.iop.org/JPhysG/31/S1623

Abstract

The structure of the neutron-rich nucleus ^{45}Ar has been investigated through the $d(^{44}\text{Ar}, ^{45}\text{Ar})p$ transfer reaction. Radioactive beam of ^{44}Ar at 10 A MeV has been provided by the SPIRAL facility at GANIL. The protons corresponding to a neutron pick-up on bound or unbound states mechanism in ^{45}Ar nuclei were detected at backward angles by the detector array MUST. The transfer-like ejectiles were detected in the SPEG spectrometer. Level scheme, spin assignments and spectroscopic factors have been deduced for ^{45}Ar and compared to shell model predictions. These parameters will be subsequently used to infer (n, γ) cross sections in the Ar isotopic chain for astrophysical purposes.

1. Introduction

Recent experimental data suggest an erosion for the $N = 28$ shell in very neutron-rich nuclei. At $N = 28$, the onset of deformation occurs through particle–hole (ph) excitations as in the $N = 20$ isotones. But contrary to the $N = 20$ region excitations across the $N = 28$ shell gap take place within the same oscillator shell, between orbitals $f_{7/2}$ and $p_{3/2}$ which are strongly connected by quadrupole interactions. Thus, even a small amount of excitations across $N = 28$ may lead to permanent quadrupole deformation. According to the β -decay [1] and Coulomb-excitation [2] experiments, quadrupole ground-state deformation develops already at $Z = 16$ four protons below the doubly magic ^{48}Ca . Study of the neutron-rich $^{40-44}\text{S}$ using the in-beam γ -spectroscopy technique [3] suggested a deformed ground state for $^{40,42}\text{S}$

and a mixed deformed configuration for ^{44}S in accordance with both the mean field [4–8] and the recent large-scale shell model calculations [9]. The role of proton collectivity contribution by the decrease of the $\pi d_{3/2}-\pi s_{1/2}$ energy difference has been pointed out also in [3, 10–12]. All these theories suggest that the erosion of the $N = 28$ shell also takes place by the lowering of the deformed intruder configurations. The recent finding of isomeric $3/2_1^-$ states in ^{45}Ar [13] and ^{43}S [14] can be interpreted as the first experimental sign in this direction. The $3/2_1^-$ state lies at around 2 MeV in ^{47}Ca , and decreases steeply below $Z = 20$ being eventually the ground state in ^{43}S . This state is a mixture of ph excitation across the $N = 28$ shell gap mainly to the $p_{3/2}$ state and coupling of the neutron hole $f_{7/2}$ to the 2^+ proton state. According to shell model calculations the first $3/2^-$ state in ^{45}Ar and ^{43}S collects 15% and 50% of $1p2h$ component, respectively. In ^{45}Ar most of the intruder strength is concentrated in the second $3/2^-$ state at 1.2 MeV, which was experimentally not observed. Determination of the energy and spectroscopic factors of the states in ^{45}Ar will clarify how the $N = 28$ shell gap evolves in neutron-rich nuclei. Information obtained through the (d, p) reaction also provides the relevant parameters for determining the neutron-capture cross-section (n, γ) in the neutron-rich Ar isotopes around/at the $N = 28$ shell closure. This is of key importance to judge whether the large overabundance of ^{48}Ca over ^{46}Ca with respect to the solar value in the EK 1-4-1 [15] inclusion of meteorite could be explained by a neutron-capture process scenario in stars.

2. Experimental methods

The transfer reaction study has been performed at GANIL with the radioactive beam of ^{44}Ar produced by the SPIRAL facility. This beam has been produced through the projectile fragmentation of a 66 A MeV ^{48}Ca primary beam of about 200 pnA intensity in a thick carbon target located at the underground production cave of SPIRAL. The isotopes of interest were produced into the target which was heated at 2000 K in order to favour their extraction. They were subsequently ionized by an ECR source to the charge 9^+ and accelerated by the cyclotron CIME up to the energy of 10 A MeV. The beam intensity of ^{44}Ar was $3 \times 10^5 \text{ s}^{-1}$, without isobaric contamination. In addition to this, a stable beam of ^{40}Ar has been produced by the same devices at similar energy in order to validate our analysis of the pick-up (d, p) reaction with a known case studied in direct kinematics [16]. The total number of ^{40}Ar and ^{44}Ar nuclei passing through the target was 3×10^9 and 10^{10} , respectively.

Neutron pick-up reactions (d, p) were induced by a $380 \mu\text{g cm}^{-2}$ thick CD_2 target. To minimize the angular divergence $\Delta\theta$ prior and after the target for a given beam emittance $(\Delta\theta \times d)$, the diameter d of the beam was chosen to be large (2 cm). The tracking of the secondary beams was achieved by a position sensitive gas filled detector CATS [17] located 11 cm downstream the target. The weak angular divergence of the beam (≤ 2 mrad) was checked by inserting temporarily another CATS detector 1.5 m upstream the CD_2 target. We have reconstructed the impact points of the nuclei on the target with an accuracy of 0.6 mm by a simple translation of the beam spot obtained with the CATS detector placed downstream of the target.

Protons were detected at backward angles (between 110 and 170°) using the eight highly segmented MUST telescopes [18]. The first stage of a MUST module consists in a $300 \mu\text{m}$ thick, $60 \times 60 \text{ mm}^2$ double sided Si-strip detector with 60 horizontal and 60 vertical strips. Each strip was backed by a lithium drifted silicon diode (Si(Li)) of approximately 3 mm thickness. The two-body pick-up reaction can then be characterized by measuring the energy and the angle of the recoiling proton detected in the MUST detector with an energy ranging from 300 keV to 6 MeV in the case of ^{45}Ar and up to 8 MeV in ^{41}Ar .

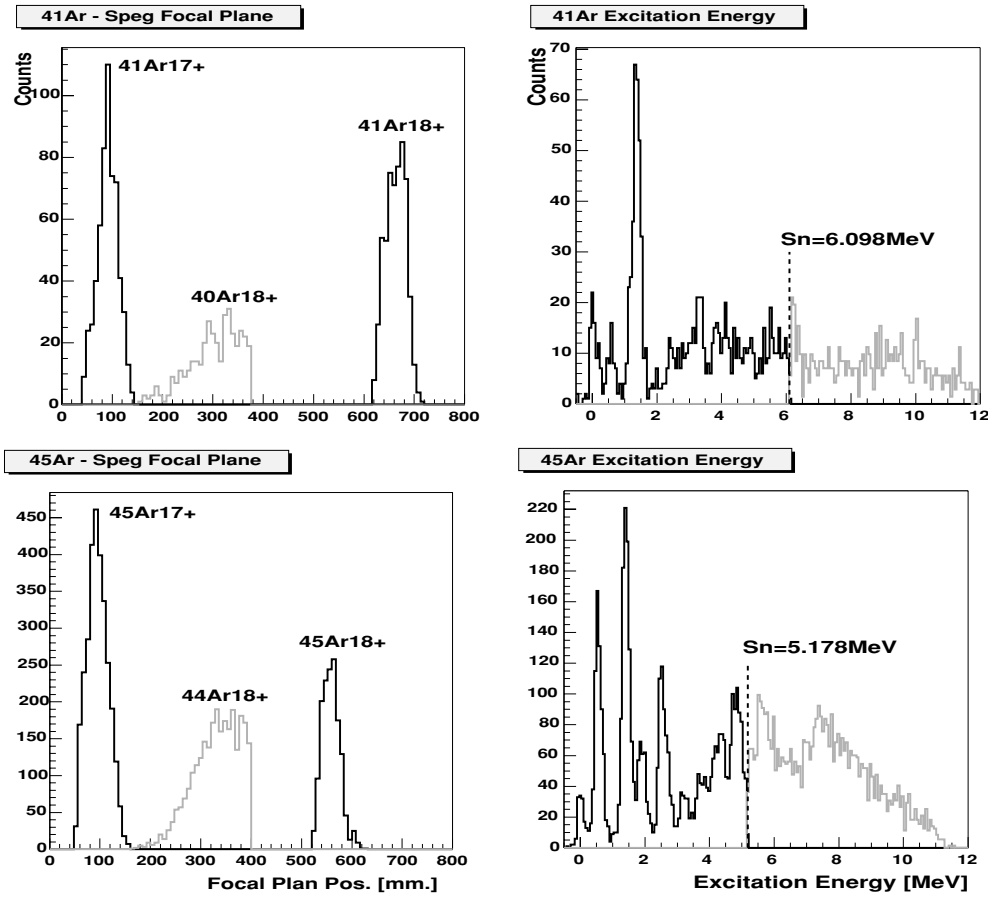


Figure 1. Left: position of the nuclei transmitted in the focal plane of SPEG for the ^{40}Ar (d, p) ^{41}Ar reaction (top) and ^{44}Ar (d, p) ^{45}Ar (bottom). The part indicated with a grey line indicates transfer above the neutron separation energy S_n . The right part shows the corresponding energy spectra.

The beam-like transfer products were selected by the SPEG spectrometer and identified at its dispersive focal plane through their position, energy loss and time of flight information. At 10 A MeV, the Ar^{9+} isotopes were not fully stripped during their interaction with the target and the CATS detector. We observed mainly two charged states $Q = 18^+$ and 17^+ in the focal plane with respective intensities of 50% and 40% over the total number of Ar (figure 1). The remaining 10% isotopes having a charge 16^+ were not transmitted. Due to its high count rate, the elastic scattering component was stopped into a thick plastic scintillator before the focal plane of SPEG. Otherwise it would have resulted in a strong electronic pile-up in the drift chambers of SPEG. Pick-up break-up component corresponding to transfer to neutron-unbound states in ^{45}Ar (^{41}Ar) has also been observed in the focal plane. This is evidenced by the detection of protons in MUST in coincidence with the low-energy tail of ^{44}Ar (^{40}Ar) nuclei in SPEG (figure 1). In order to obtain the energy spectrum of ^{45}Ar (^{41}Ar), we have used the measured proton energy and angle in MUST in the relativistic kinematics formula.

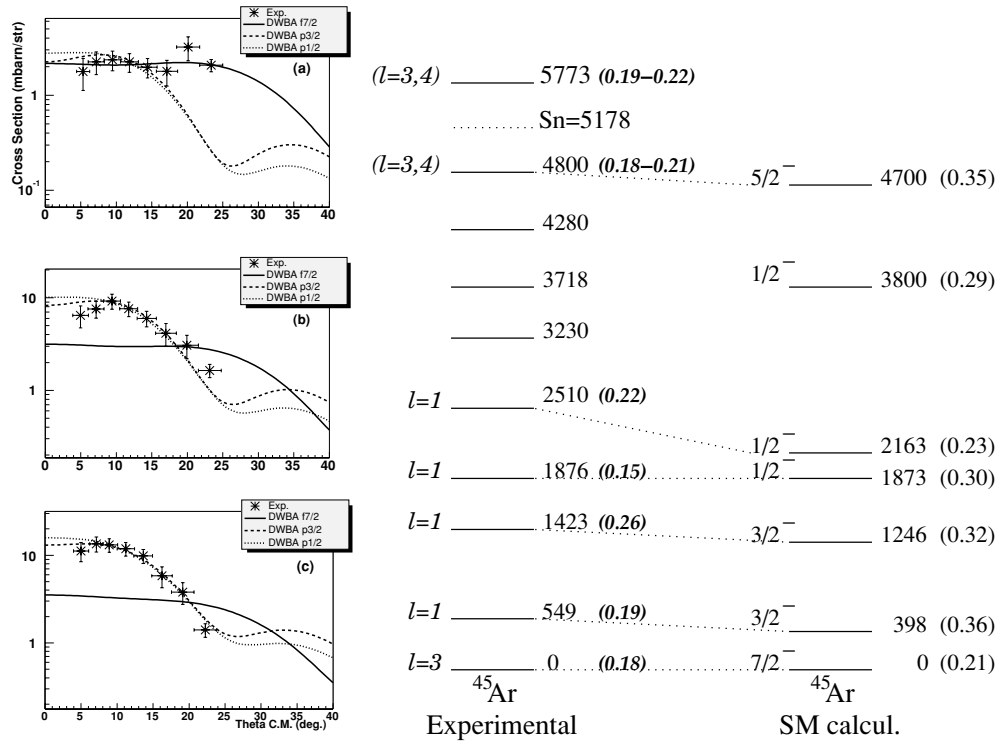


Figure 2. Left: angular distributions for the g.s. (a), first (b) and second excited states (c) in ^{45}Ar are shown in comparison to DWBA calculations assuming $\ell = 1$ or 3 distributions. Right: experimental level scheme in ^{45}Ar obtained from the present experiment is compared to shell model calculations using the ANTOINE code [22]. Calculated and preliminary experimental spectroscopic factors are indicated in parenthesis.

3. Experimental results

The energy spectra of ^{41}Ar and ^{45}Ar are shown in figure 1. Known energy peaks in ^{41}Ar are clearly visible, among which is the 1.357 MeV $3/2_2^-$ state with a large spectroscopic of 0.42(7) [16]. Energy peaks are visible in ^{45}Ar as the $3/2_1^-$ state observed by Dombrádi *et al* [13]. Well defined peaks are still visible above the S_n value. We note, however, that this spectrum cannot be exploited above 8 MeV excitation energy in ^{45}Ar because it corresponds to proton energies which are too low to be detected at the most backward angles in the MUST detector.

The angular distributions in the centre of mass have been obtained for both nuclei in order to determine the spin and spectroscopic factors of the levels. In ^{41}Ar spectroscopic factors have been deduced by fitting the experimental angular distributions to DWBA calculations using the optical potentials in the entrance ($^{40}\text{Ar}+d$) and exit channels ($^{41}\text{Ar}+p$) determined in [16]. Good agreement has been found for the three first states which have enough statistics. For the study of angular distributions in ^{45}Ar , we have used the global optical potentials given in [19] and [20] for the entrance and exit channels, respectively. All states up to 3 MeV have hitherto been studied and a clear distinction between $\ell = 3$ and $\ell = 1$ distributions is seen as shown in figure 2. They characterize neutron pick-up reaction to the f and p orbitals, respectively. Preliminary analysis shows that states located at higher energies have an $\ell = 3$ or $\ell = 4$ angular distribution which correspond to pick-up to the $f_{5/2}$ or $g_{9/2}$ orbital, respectively. A

clear energy peak is also seen about 500 keV above S_n . Experimental and hitherto calculated levels in ^{45}Ar compare well, as shown in the right part of figure 2. The energies of the two first excited states have been determined more precisely by Mrazek *et al* [21] in the β -decay study of ^{45}Cl . However their spin values could not be deduced.

4. Determination of (n, γ) cross-section from (d, p) reaction

The information provided by (d, p) experiment could be used to determine neutron-capture cross sections (n, γ) on unstable nuclei. These values play an important role in modelling the nucleosynthesis which develops in moderately neutron-rich environments, as during the freeze-out of the rapid neutron-capture process (r process) or during weak r-process scenario of typical neutron density 10^{18} cm^{-3} . From measurements achieved with stable nuclei [23] with $S_n \simeq 8 \text{ MeV}$ it was found that a drastic decrease of the neutron-capture cross section σ_n (by 2–3 orders of magnitude) occurs at the major closed shells. This is inferred mainly by the sudden decrease of the reaction Q -value immediately after a closed shell. Calculated values for nuclei in the vicinity of the valley of stability assume a predominant contribution of capture above the neutron-emission threshold where the level density is high enough to assume a statistical distribution of levels of various spin values. For neutron-rich closed-shell nuclei the level density above the S_n value is drastically reduced and statistical calculations are no longer valid. Rather a proper treatment of the few resonant states above S_n has to be made. In addition direct neutron capture (through the E1 operator) to bound states can occur when suitable orbitals with large spectroscopic factors are present. This part is dominant at $N = 28$ for the doubly magic neutron-rich ^{48}Ca nucleus due to the presence of a low-lying $3/2^-$ state ($\ell = 1$) with a large spectroscopic factor [24]. Taking into account the spin-conservation rules in the reaction the neutron is captured to the $\ell = 1$ bound state without centrifugal barrier as $\ell_n = 0$ (s-wave capture). The ratio between an s-wave ($\ell = 1$) and d-wave ($\ell = 3$) direct neutron-capture rate is approximately 10^4 at a stellar temperature of 10^9 K . In ^{45}Ar a level ($\ell = 3$ or 4) is still clearly identified above the S_n value, which indicates that a statistical treatment cannot be applied anymore. Due to its large spin value, this level does not contribute to the stellar reaction rate with a sizeable amount. The presence of low-lying bound states $3/2^-$ with sizeable spectroscopic factors (about 0.3 each) in ^{45}Ar favours direct capture cross section, as for ^{48}Ca . This leads to a drastic increase of the (n, γ) cross-section, speeding up the neutron-capture rate as compared to what normally occurs at shell closures. Important consequence of this large σ_n value is expected for explaining the abundance ratio of $^{48}\text{Ca}/^{46}\text{Ca} = 250$ in certain refractory inclusions of meteorites. These neutron-rich stable Ca isotopes could be produced during a neutron-capture and β -decay process (weak r process) by their progenitor isobars in the Ar isotopic chain. Large neutron-capture rates around $A = 46$ would reduce drastically the amount of progenitors of ^{46}Ca as the neutron-capture would quickly shift the matter flow to $A = 48$. As a consequence ^{48}Ca would be more abundant accordingly as discussed in [25].

References

- [1] Sorlin O *et al* 1993 *Phys. Rev. C* **47** 2941
- [2] Glasmacher T *et al* 1997 *Phys. Lett. B* **395** 163
- [3] Soehler D *et al* 2002 *Phys. Rev. C* **66** 054302
- [4] Werner T R *et al* 1996 *Nucl. Phys. A* **597** 327
- [5] Reinhardt P-G *et al* 1999 *Phys. Rev. C* **60** 014316
- [6] Péru S *et al* 2000 *Eur. Phys. J. A* **49** 35
- [7] Rodriguez-Guzman R *et al* 2002 *Phys. Rev. C* **65** 024304

-
- [8] Lalazissis G A *et al* 1999 *Phys. Rev. C* **60** 014310
 - [9] Caurier E *et al* 2002 *Eur. Phys. J. A* **15** 145
 - [10] Retamosa J *et al* 1997 *Phys. Rev. C* **55** 1266
 - [11] Cottle P D and Kemper K W 2002 *Phys. Rev. C* **66** 061301
 - [12] Sorlin O *et al* 2004 *Eur. Phys. J. A* **22** 173
 - [13] Dombrádi Z *et al* 2003 *Nucl. Phys. A* **727** 195
 - [14] Sarazin F *et al* 2000 *Phys. Rev. Lett.* **84** 5062
 - [15] Lee T *et al* 1978 *Astrophys. J.* **220** L21
 - [16] Sen S *et al* 1975 *Nucl. Phys. A* **250** 45
 - [17] Ottini-Hustache S *et al* 1991 *Nucl. Instrum. Methods A* **431** 476
 - [18] Blumenfeld Y *et al* 1999 *Nucl. Instrum. Methods A* **421** 471
 - [19] Wales G L and Johnson R C 1976 *Nucl. Phys. A* **274** 168
 - [20] Varner R L *et al* 1991 *Phys. Rep.* **201** 57
 - [21] Mrazek J *et al* 2004 *Nucl. Phys. A* **734** E65
 - [22] Caurier E and Nowacki F 1999 *Acta Phys. Pol.* **30** 705
 - [23] Bao Z Y and Käppeler F 2000 *At. Data. Nucl. Data Tables.* **76** 70
 - [24] Kraussmann E *et al* 1996 *Phys. Rev. C* **53** 469
 - [25] Sorlin O *et al* 2003 *C. R. Phys.* **4** 541